



ERCOFTAC Design Optimization: Methods & Applications

**International Conference & Advanced Course
Athens, Greece, March 31- April 2, 2004**

Conference Proceedings

Editors: K.C. Giannakoglou (NTUA), W. Haase (EADS-M)

ERCODO2004_205

Optimal Design of Combined Cycle Power Plants Based on Gas Turbine Performance Data

E. Bonataki
L. Georgoulis
H. Georgopoulou
K.C. Giannakoglou

⁽¹⁾⁽²⁾ Public Power Corporation, GREECE,

⁽³⁾⁽⁴⁾ National Technical University of Athens, GREECE

OPTIMAL DESIGN OF COMBINED CYCLE POWER PLANTS BASED ON GAS TURBINE PERFORMANCE DATA

Eleni T. Bonataki*, Leandros S. Georgoulis*, Hariklia Georgopoulou†,
Kyriakos C. Giannakoglou†

* Public Power Corporation,
Thermal Projects Engineering & Construction Department,
30-32 Aristotelous Str., Athens 104 33, GREECE,
Tel: (30)-210.823.15.99, Fax: (30)-210.823.01.25,
e-mail: ebonataki@dmkt.dei.gr

†National Technical University of Athens, NTUA
Lab. of Thermal Turbomachines,
P.O. Box 64069, Athens 157 10, GREECE,
Tel: (30)-210.772.16.36, Fax: (30)-210.772.37.89,
e-mail: kgianna@central.ntua.gr ,
<http://velos0.ltt.mech.ntua.gr/EASY>

Key words: Evolutionary Algorithms, Multi-objective Optimization, Combined Cycle Gas Turbine Power Plants, Gas Turbine.

Abstract. *This paper presents the design of optimal Combined Cycle Power Plants (CCGTs) by investigating the effect of Gas Turbine (GT) performance data on it. Optimization results obtained using a multi-objective evolutionary algorithm (code EASY, developed by NTUA) are compared with the performance of similar optimized plants equipped using seventeen GT modes available in the market. These are of either aeroderivative or heavy duty type, with total power output of approximately 120MW; for each one of them, the corresponding Heat Recovery Steam Generator (HRSG) parameters have been optimized using the EASY software.*

1 INTRODUCTION

Targets usually set during the design optimization of CCGT power plants differ depending on the business plan of each power producer. The power output and the efficiency of the Combined Cycle (CC) as well as the investment cost affect many plant designer's choices and determine the pay-back period of the investment. The optimization of the plant is affected by the design of the HRSG as well as the gas and steam cycles. In previous works by the authors, [1], [2], emphasis was given to the HRSG optimization without modifying any other plant component. Our objectives were to maximize the plant efficiency and minimize the investment cost; seeking the maximum CC efficiency was equivalent to designing a power plant with maximum power output, [1].

Apart from the HRSG, the GT performance affects considerably the CC design and cost. The present work investigates the role of the GT performance data, such as GT efficiency, exhaust

gas mass flowrate and temperature, to the optimization of a CCGT power plant, under the assumption that the GT power output remains fixed. The heat associated with the exhaust gases of a high-efficiency GT is low and, consequently, the steam turbine (ST) power output is expected to be lower than that of a CC plant with a low-efficiency and of the same power output GT. In view of the above, maximization of the CC power output and CC efficiency are the two (contradictory) objectives in the present study.

Since the purpose of the present work isn't to stick with purely theoretical results but mainly to include real GT performance data, seventeen GT models available in the market have been selected and the CC plants which accommodate them have been optimized using similar tools. In particular, the optimal CC plant configuration for each one of the GT models, which yields maximum power and maximum efficiency was computed and compared with theoretical optimal Pareto fronts.

The optimization tool used, code *EASY* (<http://velos0.ltt.mech.ntua.gr/EASY/>), is based on Evolutionary Algorithms (EAs). *EASY* handles three population sets, with μ parents, λ offspring and ϵ elites and employes various recombination, mutation and elitistic operators, for single- and multi-objective optimization problems. *EASY* includes and optionally employes on-line trained metamodels which, in the context of the so-called *Inexact Pre-Evaluation* (IPE) phase, screen out badly performing population members and skip a great amount of useless exact evaluations through the (usually costly) evaluation tool. The IPE possibility was not used in the present study, since the CPU cost per evaluation is very low. Constraints can be handled through penalizing the objective function values. A detailed overview of the algorithmic features of *EASY* and its additional capabilities can be found in recent publications, such as [3] and [4].

2 PROBLEM DEFINITION: THE CCGT POWER PLANT

The CCGT power plant used in the present analysis is schematically shown in fig. 1. The main components of this plant are one or more identical GTs producing a total power output of 120 MW, the same number of identical dual pressure HRSGs, one two-admission ST, the deaerator (feedwater tank), the condenser, the condensate and feedwater pumps and the generators (G1 and G2).

The power produced by the ST generator and the CC efficiency are calculated using standard thermodynamic analysis for the water/steam cycle; energy and mass balance equations are written for each and every cycle component, such as the heat exchangers, the feedwater tank, the ST and the condenser. The GT exhaust gas mass flowrate and temperature are calculated using energy and mass balance equations for the compressor and the turbine. The corresponding analysis of the combustor takes into account the combustion equations. Input quantities to the GT analysis model are the pressure ratio π_{GT} , the combustion air ratio λ_α , the compressor and turbine polytropic efficiencies ($\eta_{p,C}$ and $\eta_{p,T}$) and the generator electromechanical efficiency ($\eta_m = 97\%$). Two levels of polytropic efficiencies for each component have been used, namely $\eta_{p,C} = 85\%$ and 90% for the compressor and $\eta_{p,T} = 70\%$ and 75% for the turbine. For the ST and the generators, the isentropic $\eta_{is,ST-HP} = 90\%$ (for the high-pressure ST) and $\eta_{is,ST-LP} = 87\%$ (for the low-pressure ST) efficiencies as well as the mechanical ($\eta_{m,ST} = 95\%$) and electrical ($\eta_{el,ST} = 98\%$) ones are all known and fixed. Known extraction pressure (2.5 bar) from the LP part of the ST at position *ex*, fig. 1, and condenser vacuum (45 mbar, position 22) are also

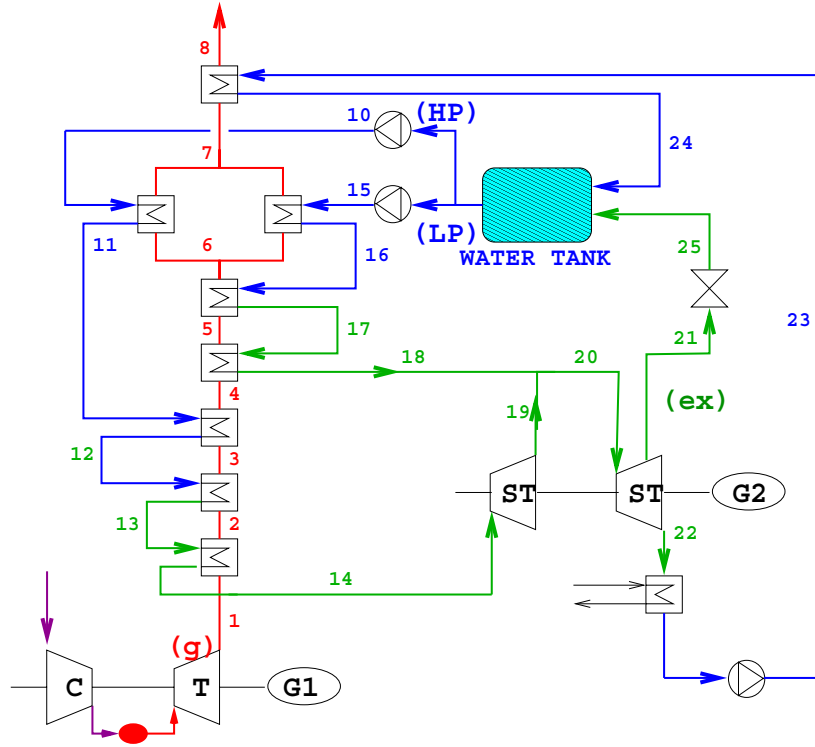


Figure 1: CCGT power plant configuration with a dual pressure HRSG. Though a single GT unit is shown, the 120MW GT may consist of more than one units.

considered. The thermodynamic properties of water, steam and exhaust gases are modeled, [5]. We recall that a fixed GT (or GTs) total power output (equal to 120 MW) is imposed. The design variables used are listed below along with their lower and upper bounds (given in brackets) for the most important among them. It should be noted that some of the free-to-vary temperatures are defined as differences from other fixed or varying temperatures computed during the power plant analysis. Design variables are:

- the GT pressure ratio $\pi_{GT} = [12, 30]$,
- the GT air combustion ratio $\lambda_{\alpha} = [2.8, 4]$
- the HP steam pressure $p_{HP} = [20, 100 \text{ bar}]$,
- the LP steam pressure $p_{LP} = [2, 15 \text{ bar}]$,
- the superheated steam temperature at the exit of the HP branch of the HRSG (position 14), expressed as difference from the GT exhaust gas temperature (position 1),
- the feedwater temperature at the inlet to the HP evaporator (position 12),
- the feedwater temperature at the exit from the first HP economizer (position 11),

- the feedwater temperature at the inlet to the LP evaporator (position 16),
- the superheated LP steam temperature (position 18), expressed as the difference from the saturated steam temperature,
- the steam pressure at the inlet to the water tank (position 25), [1.1, 2.0 bar],
- the percentage of exhaust gases mass flowrate passing through the LP economizer [10%, 45%],
- the exhaust gas temperature at the inlet to the condensate preheater (position 7),
- the HRSG exhaust (position 8) gas temperature [103, 110°C]

The two objectives of the optimization procedure are: (a) maximization of the CC power output P_{CC} and (b) maximization of the CC efficiency (η_{CC}). A number of operational constraints are imposed, most of them for the purpose of designing feasible heat exchangers. Also, the turbine inlet temperature (TIT) is not allowed to exceed 1350°C and the GT exhaust gas temperature (EGT , position 1) should be less than 550°C. Should any constraint be violated, a penalty value which is proportional to the degree of constraint violation, is computed. Exponential penalty functions are used. The cost values for both objectives are multiplied by these penalties.

3 ANALYSIS OF THE CC POWER PLANT

In a previous work by the authors, [1], the CCGT optimization was carried out with fixed GT operational data; in [1], the maximization of η_{CC} was linked only to the ST power output, by focusing on the design of optimal HRSG.

In contrast, in the present paper only the GT power output (P_{GT}) is considered to be fixed and parameters such as the GT efficiency (η_{GT}) and the GT exhaust gas mass flowrate (\dot{m}_{GT}) and temperature (EGT) are free to vary; any (feasible) set of values these parameters may take on corresponds to different P_{CC} and η_{CC} values. Setting the maximization of P_{CC} and η_{CC} as objectives, Pareto fronts of optimal solutions are computed, using the *EASY* software. The front members should be considered as compromises between the two extreme configurations, namely the one with (low- P_{CC} , high- η_{CC}) and that with (high- P_{CC} , low- η_{CC}).

Objectives, design variables, fixed parameters and constraints have all been described in the previous section. The only two fixed parameters that take on more than one values are $\eta_{p,C}$ and $\eta_{p,T}$; for this reason, all computations have been repeated three times, for $(\eta_{p,C}, \eta_{p,T}) = (90\% - 70\%)$, $(85\% - 75\%)$ and $(90\% - 75\%)$ respectively, yielding different fronts of optimal solutions. As it will be demonstrated below, the GT performance data calculated using these three selected pairs of values are representative of the performance of real machines.

One of the major concerns of the present study is the comparison of theoretical optimization results with the performance of similar CCGT power plants built using GT models available in the market. Seventeen GT models, which are representative of the GT technology evolution during the last decade, are listed in Table 1. Their power output is close to either 30, 40, 60 or 120MW, so they are going to be used in combinations of four, three, two units or as a single unit, respectively. By doing so, the total GT power output is close (but not equal) to 120MW; this is why, in the sake of fairness during the comparison of results, the CC power output divided

by the GT one will be used instead of the CC power itself. It is interesting to note that the η_{GT} and π_{GT} values of the seventeen GT models vary considerably, ranging from 32% to 41.4% and 12 to 29, respectively.

No.	GT Power Output (kW)	GT Efficiency (%)	Pressure Ratio	Exhaust Gas Mass Flowrate (kg/s)	Exhaust Gas Temperature ($^{\circ}C$)	Number of Units
1	42100	32,06	12,2	141,33	547,8	3
2	126100	33,79	12,6	418,55	542,8	1
3	30000	31,98	15,0	108,16	532,8	4
4	116500	33,95	15,5	400,83	530,0	1
5	63000	35,20	16,1	192,23	531,0	2
6	57000	34,00	17,6	200,41	508,0	2
7	29060	35,99	18,0	91,25	518,0	4
8	42300	36,26	19,0	117,25	569,4	3
9	43000	37,03	20,0	122,70	546,0	3
10	29500	37,68	21,5	95,89	493,3	4
11	32120	39,31	21,5	94,53	503,3	4
12	30349	39,78	21,5	84,48	499,4	4
13	30281	39,14	22,1	84,53	513,3	4
14	29244	35,44	22,6	87,94	519,4	4
15	30280	38,13	22,7	87,25	515,0	4
16	42984	41,39	27,6	128,16	440,0	3
17	41711	40,75	29,3	126,97	447,8	3

Table 1: Performance data for seventeen GTs available in the market. The last column denotes the number of units used to produce approximately 120MW (for instance, three units No. 1, producing 42100kW each, will be used in the CCGT power plant and so forth).

For each one of the above models, the analysis software was slightly modified. The algorithm by-passed the part of the analysis which computes the GT performance data using known π_{GT} , λ_{α} , $\eta_{p,C}$ and $\eta_{p,T}$ values. Data listed in Table 1 have been used instead. The results of the seventeen computations (each computation corresponds to a single point) along with the three Pareto fronts that correspond to the three pairs of compressor and turbine polytropic efficiencies are shown in fig. 2. The three Pareto fronts can be considered as three overlapping parts of a “global” front; the $(\eta_{p,C}, \eta_{p,T}) = (90\% - 75\%)$ front covers the low- P_{CC} /high- η_{CC} part of the global front (top-left) whereas the $(90\% - 70\%)$ one lies on its high- P_{CC} /low- η_{CC} part (bottom-right). The majority of the seventeen points are close to the Pareto fronts, though clearly dominated by their members. Only GT No. 8 dominates a part of the fronts and this is attributed to the fact that $EGT = 569^{\circ}C$ is much higher than the upper limit of $550^{\circ}C$ used as one of the constraints. Further insight can be gained by plotting other quantities in terms of one of the objectives. For instance, in fig. 3, η_{GT} is plotted in terms of P_{CC} . Direct comparison of figs. 2 and 3 indicates that the higher the GT efficiency η_{GT} , the higher is the optimal CC efficiency η_{CC} . It must be stressed that the seventeen GTs have η_{GT} close enough

to the theoretical fronts and this substantiates the selection of the three $(\eta_{p,C}, \eta_{p,T})$ sets used in the computations.

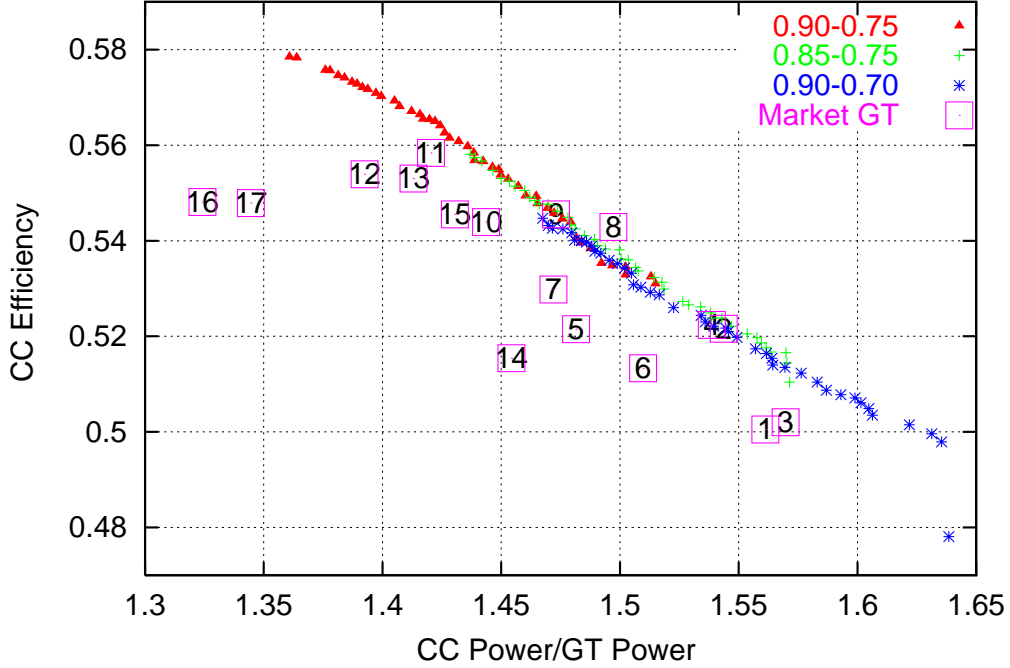


Figure 2: Pareto fronts for the three $(\eta_{p,C}, \eta_{p,T})$ sets of values along with single point representation of the seventeen market GTs, plotted on the objectives' plane.

In figs. 4 and 5, the optimal solutions' \dot{m}_{GT} and EGT are plotted in terms of the P_{CC} . For GTs with higher polytropic efficiencies (90% – 75%), EGT ranges from $520^{\circ}C$ to $550^{\circ}C$. The other two fronts almost exclusively reach the upper bound of $550^{\circ}C$. As already stated, only GT No. 8 exceeds the upper EGT limit of $550^{\circ}C$. \dot{m}_{GT} is inversely proportional to η_{CC} and proportional to P_{CC} .

Next, we provide some comments on the different performances of some of the seventeen GTs. This discussion is by no means exhaustive; the seventeen points have been classified and some distinct cases are further discussed. The η_{CC} value for most of the GT models are close enough to the Pareto fronts though dominated by the fronts points since their EGT and η_{GT} is lower, fig. 5. For instance, GT No. 10 is a model dominated by the front (fig. 2) but with satisfactory η_{CC} and P_{CC} values. With reasonably good η_{GT} , No. 10 behaviour exhibits a balance between a very low EGT and high \dot{m}_{GT} . By contrast, the performance of No. 14 is much worse than the Pareto front. This is attributed to the low GT efficiency and EGT whereas \dot{m}_{GT} is not that high compared to the Pareto solutions. Finally, the extremely low EGT of models No. 16 and 17 ($440^{\circ}C$ and $448^{\circ}C$, respectively, fig. 5) is the main reason for their bad performance compared to the Pareto solutions, fig. 2.

The three fronts shown in figs. 2, 3, 4 and 5, for the three value sets of $(\eta_{p,C}, \eta_{p,T})$, share some common parts; so, they give the impression of being parts of the same front. This is not

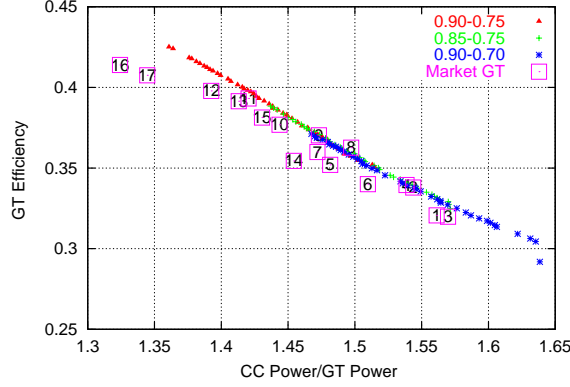


Figure 3: Pareto fronts along with single point representation of the seventeen GTs available in the market, plotted on the $\eta_{GT}-P_{CC}$ plane.

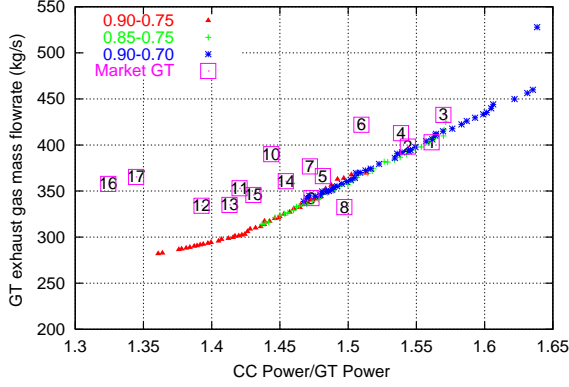


Figure 4: Optimal Pareto front points and CCGT designs with the GTs available in the market, plotted on the \dot{m}_{GT} and P_{CC} plane.

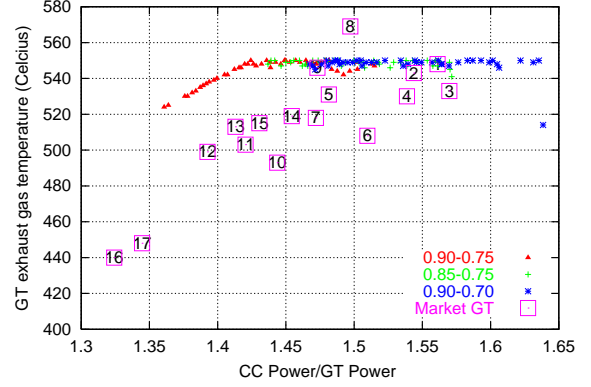


Figure 5: Optimal Pareto front points and CCGT designs with the GTs available in the market, plotted on the EGT and P_{CC} plane.

the case for π_{GT} and TIT plots, figs. 6 and 7, where three well separated fronts can be seen. The same point on the Pareto fronts of fig. 2 can be obtained using different sets of polytropic efficiencies. For instance, a Pareto optimal solution with $\eta_{CC} = 0.54$, fig. 2, can be obtained with either $(\eta_{p,C}, \eta_{p,T}) = (90\% - 75\%)$ or $(90\% - 70\%)$. The high- $\eta_{p,T}$ case yields $\pi_{GT} = 13.8$ and $TIT = 1155^\circ C$ whereas the low- $\eta_{p,T}$ case yields $\pi_{GT} = 27.2$ and $TIT = 1287^\circ C$. Thus, by increasing $\eta_{p,T}$ from 70% to 75%, π_{CC} falls from 27.2 to 13.8 and TIT from $1287^\circ C$ to $1155^\circ C$, for the same η_{GT} , \dot{m}_{GT} and EGT .

In fig. 8, the GT efficiency is plotted in terms of π_{GT} . As stated elsewhere, all of the seventeen GTs fall within the range of polytropic efficiencies used in the optimization. The majority of them coincide with the second curve, $(\eta_{p,C}, \eta_{p,T}) = (85\% - 75\%)$.

Figs. 9 and 10 show the steam (HP and LP) pressure levels in the HRSG. The high pressure remains close to the upper bound (100bar) imposed in the optimization while the low pressure is around 6bar for the case with polytropic efficiencies (90% - 70%) and most of the other two fronts points are around 8bar. For the seventeen GTs, the high pressure is very close to the

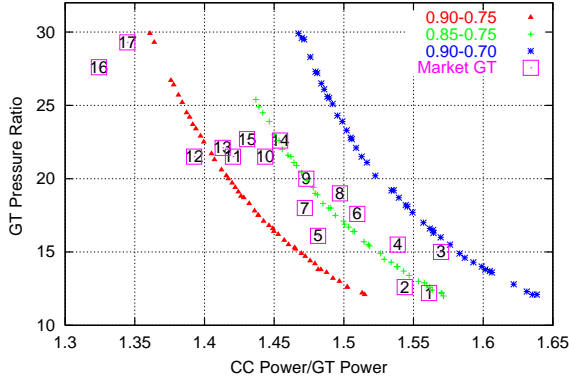


Figure 6: Optimal Pareto front points and CCGT designs with the GTs available in the market, plotted on the π_{GT} and P_{CC} plane.

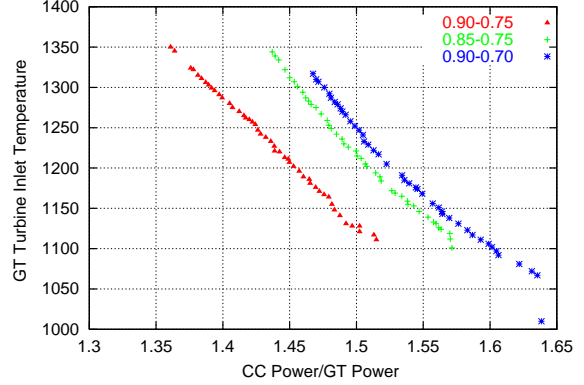


Figure 7: Optimal Pareto front points plotted on the TIT and P_{CC} plane.

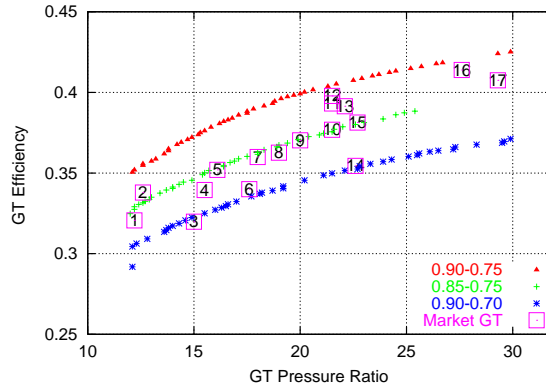


Figure 8: Optimal Pareto front points and CCGT designs with the GTs available in the market, plotted on the η_{GT} and π_{GT} plane.

upper bound of 100bar , except for No. 16 and 17. For the latter, the low (compared to the Pareto solutions) EGTs (440°C and 448°C) result to HP steam pressures of about 50bar and 70bar , respectively. Due to the above, the ST power output and η_{CC} are low. The LP steam pressures of the seventeen GTs lie in the area defined by the three optimal curves.

The exhaust gas-water/steam temperature along the HRSG vs. the exchanged heat ($Q - T$ diagram) for the two endpoints of a Pareto front are shown in figs. 11 and 12. Fig. 11 corresponds to CC power output of 181.6MW and $\eta_{CC} = 52.9\%$ and this is the Pareto point with maximum power output. Fig. 12 corresponds to $P_{CC} = 163.5\text{MW}$ and $\eta_{CC} = 57.9\%$ and this is the Pareto point with maximum efficiency.

4 CONCLUSIONS

The spreadwise use of evolutionary optimization methods for the design of optimal CCGT power plants is known and many relevant papers are available in the literature. Here, we focused on the GT performance data and we utilized EAs not only for obtaining optimal configurations

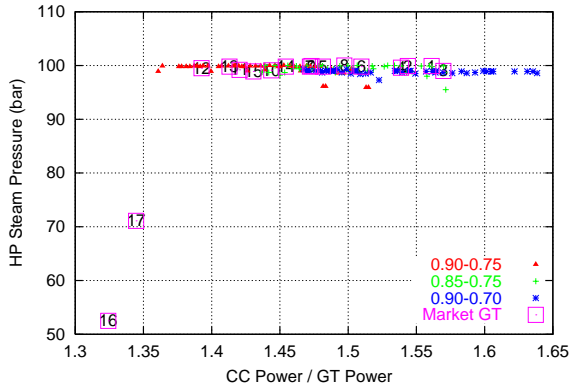


Figure 9: Optimal Pareto front points and CCGT designs with the GTs available in the market, plotted on the HP steam pressure value and π_{GT} plane.

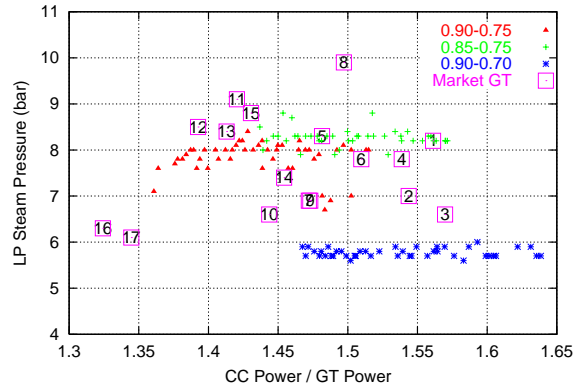


Figure 10: Optimal Pareto front points and CCGT designs with the GTs available in the market, plotted on the LP steam pressure value and π_{GT} plane.

but, also, for investigating and understanding the effect of GT performance on the two objectives used, namely maximum CC power output and maximum CC efficiency. To proceed beyond a simple theoretical study, the same optimization tool was used to optimally configure CCGT plants which use GT models available in the market. Our studies confirmed that the GT efficiency is proportional to the CC efficiency and inversely proportional to the CC power output. The majority of the market GTs perform similarly to the theoretical optimal solutions; although they might have different pressure ratios or GT exhaust gas mass flowrates or temperatures.

In industrial outfits, studies such as the present one and tools such as the ones used herein can be used at the decision making level.

REFERENCES

- [1] Bonataki, E.T., Giannakoglou, K.C., An Automated Tool for Single- and Multi Objective Optimization for Redesigning Combined Cycle Gas Turbine Power Plants, Proceedings of the Fourth GRACM Conference on Computational Mechanics, Patras, Greece, June 2002.
- [2] Bonataki, E.T., Giotis A.P., Giannakoglou, K.C., Multi-Objective Design of Optimal Combined Cycle Power Plants with Supplementary Firing, EUROGEN 2003, Barcelona, Spain, Sep. 15-17, 2003.
- [3] Giannakoglou, K.C., Design of Optimal Aerodynamic Shapes using Stochastic Optimization Methods and Computational Intelligence, Progress in Aerospace Sciences, 38, pp. 43-76, 2002.
- [4] Karakasis, M., Giotis, A.P., Giannakoglou, K.C., Efficient Genetic Optimization Using Inexact Information and Sensitivity Analysis. Application in Shape Optimization Problems, ECCOMAS CFD Conference 2001, Swansea, Wales, 2001.
- [5] Ganapathy, V., Basic Programs for Steam Plant Engineers, Marcel Dekker, Inc., ISBN-0-8247-7489-2.

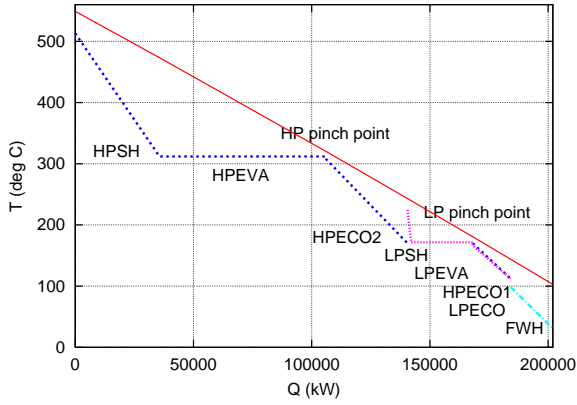


Figure 11: $Q - T$ diagram for the optimal solution with the highest power output ($P_{CC} = 181.6MW$ and $\eta_{CC} = 52.9\%$).

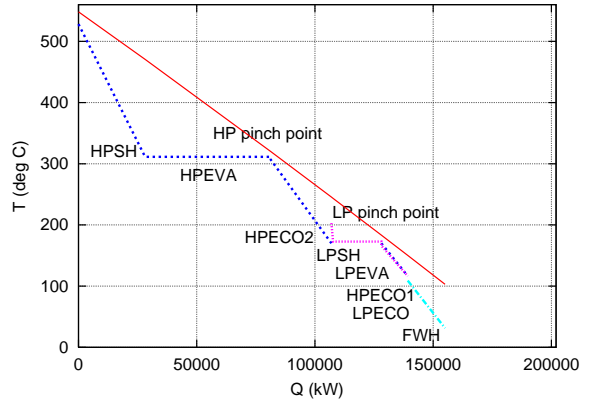


Figure 12: $Q - T$ diagram for the optimal solution with the highest CC efficiency ($P_{CC} = 163.5MW$ and $\eta_{CC} = 57.9\%$).